American Journal of Pathology, Vol. 169, No. 1, July 2006

DOI: 10.2353/ajpath.2006.051238

Cell Injury, Repair, Aging and Apoptosis

L-Asparaginase-Induced Antithrombin Type I Deficiency

Implications for Conformational Diseases

David Hernández-Espinosa,* Antonia Miñano,* Constantino Martínez,* Elena Pérez-Ceballos,* Inmaculada Heras,* José L. Fuster,† Vicente Vicente,* and Javier Corral*

From the Centro Regional de Hemodonación, Universidad de Murcia; and the Servicio de Oncología Pediátrica,† Hospital Virgen de la Arrixaca, Murcia, Spain*

Serpinopathies, a group of diseases caused by mutations that disrupt the structurally sensitive serpins, have no known acquired cause. Interestingly, L-asparaginase treatment of acute lymphoblastic leukemia patients causes severe deficiency in the serpin antithrombin. We studied the consequences of this drug on antithrombin levels, activity, conformation, and immunohistological and ultrastructural features in plasma from acute lymphoblastic leukemia patients, HepG2 cells, and plasma and livers from mice treated with this drug. Additionally, we evaluated intracellular deposition of α1-antitrypsin. L-Asparaginase did not affect functional or conformational parameters of mature antithrombin; however, patients and mice displayed severe type I deficiency with no abnormal conformations of circulating antithrombin. Moreover, L-asparaginase impaired secretion of antithrombin by HepG2 cells. These effects were explained by the intracellular retention of antithrombin, forming aggregates within dilated endoplasmic reticulum cisterns. Similar effects were observed for α1-antitrypsin in plasma, cells, and livers, and intracellular aggregates of additional proteins were observed in frontal cortex and pancreas. This is the first report of a conformational drug-associated effect on serpins without genetic factors involved. L-Asparaginase treatment induces severe, acquired, and transient type I deficiency of antithrombin (and α1-antitrypsin) with intracellular accumulation of the nascent molecule, increasing the risk of thrombosis. ***(Am J Pathol 2006, 169:142–153; DOI: 10.2353/ajpath.2006.051238)***

Venous thromboembolism is a multifactorial disorder in which genetic and acquired risk factors may interact to determine the occurrence of the thrombotic event. Throughout the last 30 years, a significant effort has been done to determine inherited risk factors associated with venous thrombosis. But even including low-risk polymorphisms up to 50% of cases have no identified genetic risk factors. Much more effort is required to identify other factors causing a transient hypercoagulable state that could increase the risk of thrombosis and their underlying mechanisms.

Antithrombin is the most important endogenous anticoagulant. Deficiency of this serpin significantly increases the risk of venous thrombosis, and homozygous deficiency is lethal.[1] As for any other serpin, a flexible structure of antithrombin is essential for its inhibitory action, which leads to an irreversible destruction of the target proteases. However, this structural flexibility also makes serpins, and particularly antithrombin, especially vulnerable to conformational changes with relevant functional or pathological consequences.[2] Thus, the modification of just a single amino acid in structurally sensitive regions or any other factor able to disturb the complex network of interactions in the whole molecule may produce overall conformational changes that affect all of the functions of antithrombin, including its inhibitory activity and its heparin-binding affinity. But most importantly, such conformational changes can result in a loss of stability and facilitate the formation of intermolecular linkages and its subsequent intracellular retention. Accordingly, some cases of venous thrombosis have been included in the group of conformational diseases.[3] Antithrombin deficiency is caused by a range of rare mutations associated with a strong thrombotic risk (T. Bayston, D. Lane: Antithrombin mutation database. Department of

Supported by the Fundación Séneca (00583/PI/04, SAF2003-00840).

Accepted for publication March 30, 2006.

Address reprint requests to Dr. Javier Corral, Centro Regional de Hemodonación, C/Ronda de Garay s/n, Murcia 30003 Spain. E-mail: jcc@um.es.

Haematology, Imperial College Faculty of Medicine, Charing Cross Hospital Campus, Hammersmith, London, UK. *http://www1.imperial.ac.uk/medicine/about/divisions/is/haemo/antithrombin/default.html*), some with demonstrated conformational effect.[4] Acquired antithrombin deficiency, also associated with an increased incidence of thromboembolic events, occurs as a result of decreased production, increased consumption, or increased renal loss. However, few factors have been identified to cause transitory deficiency of antithrombin.

L-Asparagine amido hydrolase, E.C. 3.5.1.1 (ASNase), is a bacterial enzyme that produces aspartic acid and ammonia by asparagine hydrolysis.[5] This enzyme is used as an anti-neoplastic agent in acute lymphoblastic leukemia (ALL) chemotherapy. Unfortunately, this treatment causes a severe deficiency of antithrombin that might explain the associated high incidence of venous thromboembolism (up to 36.7% in some series).[6] A recent and extensive study supports that patients who received ASNase had a 4.9-fold increased risk of thrombosis in comparison with those who did not (95% CI, 1.5 to 16.0).[7] Moreover, the fatality rate attributable to thrombosis was 0.8%.[7] However, the mechanism responsible for the decrease of plasma antithrombin caused by ASNase remains elusive.

Materials and Methods

Patients

ALL patients ($n = 19$) after induction therapy received intravenous ASNase (Elspar; Merck and Co., Whitehouse Station, NJ) at 10,000 IU/m^2 on days 9 to 11, 16 to 18, and 23 to 25 of the induction chemotherapy. Additionally, patients received intravenous prednisolone at 60 mg/m^2 on days 1 to 27 and 30 mg/m^2 on days 28 to 35; intravenous vincristine at 1.5 mg/m^2 on days 8, 15, 22, and 28; intravenous daunorubicin at 30 mg/m^2 on days 8 and 15; intravenous cyclophosphamide at 1000 mg/m^2 on day 22; and intrathecal therapy (methotrexate, ARA-C, and hydrocortisone) on days 1 and 22. Venous blood from ALL patients under ASNase treatment was collected into 10 mmol/L trisodium citrate tubes. Fresh plasma from these samples was obtained by centrifugation and immediately aliquoted and stored at −70°C until the moment of use. Two of these patients developed venous thromboembolic events. As a control, we generated a pool of citrated plasma from 100 healthy blood donors. The University of Murcia ethics committee approved the protocol, and informed consent was obtained from patients or their relatives.

In Vitro Studies

Venous blood from healthy blood donors ($n = 4$) was anti-coagulated with 10 mmol/L trisodium citrate. Fresh plasma from these samples was obtained by centrifugation and immediately stored in aliquots at −70°C. Plasma samples were incubated with ASNase at either 70 or 700 IU/ml (the amount and a 10 times higher amount than that expected in plasma of patients treated with this drug) up to 72 hours. Similar studies were performed with purified human antithrombin obtained from commercial concentrates of therapeutic use (Kybernin-P; Aventis Behring, Strasbourg, France).

Cell Culture Studies

Semiconfluent cultures of the human hepatoma HepG2 cell line cultured in Dulbecco's modified medium (GibcoBRL, Paisley, UK) plus 10% fetal calf serum (GibcoBRL) were extensively washed with phosphate-buffered saline (PBS) and incubated in fetal calf serum-deprived Dulbecco's modified medium (GibcoBRL) and treated with 70 IU/ml ASNase (in sterile PBS). The same volumes of sterile PBS were added to the medium of control cells. Cell culture media samples from these groups were collected (250 μl) at 24 hours after treatment and frozen at −70°C until the moment of use. Cells were either fixed in 4% PBS-formaldehyde or lysated for immunoblotting or immunoprecipitation purposes. Experiments ($n = 6$) were performed in sixtuplicate.

Mouse Model

Non-inbred Swiss (ICR CD-1) male mice were intraperitoneally injected with 10,000 IU/m^2 ASNase ($n = 8$) for 2 consecutive days. Controls were intraperitoneally injected with sterile PBS ($n = 10$). Venous blood samples (10 μl) were collected on days 0, +1, and +2 after treatment into 10 mmol/L trisodium citrate-containing tubes. Mice were sacrificed on day +2. Livers were finely dissected and either fixed in 4% PBS-formaldehyde for histolopathology purposes or 4% glutaraldehyde for electron microscopy purposes, or frozen in liquid nitrogen for immunoblotting purposes. A control pool of citrated plasma from 10 untreated mice was generated. The animals were kept under standardized conditions, and tap water and mouse chow were provided *ad libitum*. All experimental procedures were performed in accordance with the University of Murcia approved institutional animal care guidelines.

Determination of Anti-Factor Xa Activity and Antigenic Levels of Antithrombin

Antithrombin activity in plasma was determined using a commercial chromogenic (S-2765) anti-factor Xa (FXa) assay with heparin (Instrumentation Laboratory, Milano, Italy). Antithrombin antigen in plasma samples (from patients and mice) and medium samples were measured by enzyme-linked immunosorbent assay and electro-immunodiffusion (Laurell). Unless indicated, values were expressed as percentage of the results observed in the respective control plasma pools (100%).

Detection of Conformational Variants of Antithrombin

Sodium dodecyl sulfate-polyacrylamide gel electrophoresis (SDS-PAGE) was performed in 8% (w/v) polyacrylamide gels, running purified antithrombin or plasma (750 ng of antithrombin) and cell or liver lysates (40 μg), as previously described.[8] Additionally, nondenaturing PAGE was performed as indicated elsewhere, with minor variations.[9] Addition of 6 mol/L urea to the native gel allows differentiation of the native and latent forms of antithrombin, as reported.[10] Briefly, purified antithrombin (0.2 to 25 μg) and plasma from patients (1 to 2 μl) were run in nondenaturing gels (with or without 6 mol/L urea). Finally, the features of intracellular antithrombin in HepG2 cells were also analyzed using two-dimensional electrophoresis.

Plasma from patients, mice, and cell lysates were blotted onto polyvinylidene difluoride membranes and immunostained with goat anti-human antithrombin or anti-human α-1 antitrypsin polyclonal antibodies (Dako Diagnostics, Glostrup, Denmark), followed by rabbit anti-goat IgG-horseradish peroxidase conjugate (Amersham Biosciences Ltd., Little Chalfont, UK). Both primary antibodies are able to recognize both mouse proteins given the high degree of homology between human and mouse. Densitometric analysis of bands was performed using the Quantity-One software (Bio-Rad, Denver, CO). Purified antithrombin was immunodetected or stained with Coomassie.

Crossed Immunoelectrophoresis

Antithrombin affinity to heparin was evaluated by means of bidimensional electrophoresis with heparin, using the reagents and following the conditions previously described by our group.[11]

Detection of Antithrombin in HepG2 Cells and Livers of Mice Treated with ASNase

Livers were weighed, minced, and homogenized into 10× volume of ice-cold lysis buffer [10 mmol/L Tris-HCl, 0.5 mmol/L dithiothreitol, 0.035% SDS, 1% Triton X-100, 50 μmol/L protease inhibitor cocktail (Sigma-Aldrich, Poole, UK)]. The homogenate was centrifuged at 13,000 rpm for 10 minutes, supernatants were kept and the pellets were resuspended into 5× volume of lysis buffer. These samples were stored at −80°C until the moment of use. Similarly, HepG2 cells were extensively washed with sterile PBS and then lysed with 500 μl of lysis buffer and stored at −80°C until the moment of use. Bradford assays (Bio-Rad) were performed to determine the protein concentrations.

To detect antithrombin, supernatants (40 μg) and pellets (40 μg) of liver and cell extracts (40 μg) were boiled for 5 minutes in Laemmli buffer with 1 mmol/L dithiothreitol before electrophoresis and loaded into denaturing gels. Additionally, HepG2 lysates were immunoprecipitated with a rabbit anti-human antithrombin polyclonal antibody (10 μg, Dako Diagnostics) for 16 hours. Sixty μl of 50% slurry agarose-immobilized protein G (Invitrogen Co., Carlsbad, CA) containing 2.5% bovine serum albumin were added, and the suspension was rotated for an additional 2 hours at 4°C. Agarose beads were washed five times in lysis buffer. Protein was eluted with 0.1 mol/L glycine-HCl, pH 2.5 and buffered with 100 mmol/L Tris, pH 7.5. Eluate (50 μl) was resuspended in two-dimensional electrophoresis solubilization buffer (160 μl) consisting of 9 mol/L urea, 3% CHAPS, 2% Triton X-100, 20 mmol/L dithiothreitol, and 0.5% ampholytes. Immobilized pH gradient (IPG) strips (ReadyStrip IPG 11 cm, pH 4.7 to 5.9 linear; Bio-Rad) were passively rehydrated overnight with protein solution. Isoelectric focusing of proteins was performed using the following step gradient: 500 V for 1 hour, 1000 V for 1 hour, and 8000 V until a total of 35,000 V-hours had been achieved (Protean IEF Cell, Bio Rad). After isoelectric focusing, strips were equilibrated in buffer containing 7 mol/L urea, 2% SDS, 375 mmol/L Tris (pH 8.8), and 10% glycerol plus either 50 mmol/L dithiothreitol for reduction or 100 mmol/L iodoacetamide for alkylation. Equilibrated IPG strips were loaded onto a 10% acrylamide gel and electrophoresed. Gels were blotted to polyvinylidene difluoride membranes and immunostained with goat anti-human antithrombin polyclonal antibody (Sigma-Aldrich), as indicated before.

Histological and Histopathological Analyses

Paraffin-embedded liver, pancreas, and frontal cortex sections (4 μm) were stained with hematoxylin (Panreac, Catelar del Vallès, Spain), counterstained with eosin (Panreac), dehydrated, and mounted in Dpex mounting medium (Panreac) for light microscopy observation. To detect intracellular β-sheet-mediated deposits of proteins, Congo Red (Merck, Darmstadt, Germany) staining was performed. Glycoproteic deposits were assessed by the appearance of periodic acid Schiff-positive deposits (Panreac). Cell viability was assessed by Hoechst staining (Sigma-Aldrich) and numbers of nuclei counted in eight random ×40 fields under blue fluorescence (excitation, 365 nm; emission, 465 nm).

For antithrombin and α1-antitrypsin immunohistochemistry purposes, a peroxidase-anti-peroxidase technique was performed. Briefly, sections were rinsed and endogenous peroxidase inhibited. Sections were blocked in blocking solution [0.1% Tween-Tris-buffered saline (TBS), 10% fetal calf serum, 5% bovine serum albumin] for 30 minutes and incubated with rabbit anti-human antithrombin polyclonal antibody (1:1000, Dako Diagnostics) or rabbit anti-human α1-antitrypsin polyclonal antibody (1:250, Dako Diagnostics) for 90 minutes. Then, sections were washed three times in 0.1% Tween-TBS and incubated with biotin-labeled anti-rabbit secondary antibody (1:250; Vector Laboratories, Burlingame, CA) and signal-amplified with an ABC kit (Vector Laboratories). Sections were then washed twice in 0.1% Tween-TBS, once with TB, rinsed, developed with 3,3′-diaminobenzidine (0.5 mg/ml) (Sigma-Aldrich) in 50 mmol/L TB (pH 7.6), counterstained with hematoxylin, dehydrated, and mounted.

HepG2 hepatoma cells were histologically stained with the same techniques used for liver sections although no dehydration was performed. Mounting was performed in Vectashield mounting medium (Vector Laboratories). Antithrombin and α1-antitrypsin immunofluorescence of HepG2 cells was assessed. Briefly, cells were rinsed with PBS and blocked with blocking solution (0.3% Tween-PBS, 10% fetal calf serum, 5% bovine serum albumin). After this step, cells were incubated with rabbit anti-human antithrombin or anti-α1-antitrypsin polyclonal antibodies (1:1000 and 1:250, respectively; Dako Diagnostics) for 90 minutes and washed three times in 0.1% Tween-PBS. Cells were then incubated with a fluorescein-labeled anti-rabbit IgG secondary antibody (1:250, Vector Laboratories) for 1 hour, washed three times in 0.1% Tween-PBS, mounted in Vectashield mounting medium (Vector Laboratories) and observed using green fluorescence (excitation, 488 nm; emission, 530 nm).

Electron Microscopy Studies

Fixed samples of livers from ASNase-treated or control mice (4% glutaraldehyde) were dehydrated in sequential gradients of ethanol. Samples were then infiltrated with increasing concentrations of LR White resin (Merck). Polymerization of the resin was performed under oxygen-free conditions for 24 hours at 50°C. Ultrathin section were cut by using a Leica ultramicrotome (Leica Mycrosystems, Heidelberg, Germany) at 50 nm onto copper grids (for ultrastructural analysis) or nickel grids (for immunogold labeling). Copper grid sections were postfixed with osmium tetroxide and then stained with uranyl acetate and lead citrate. Ultrastructural morphology of mouse liver was analyzed using an EM-10 Zeiss transmission electron microscope (Zeiss, Oberkochen, Germany).

A colloidal gold immunostaining technique for antithrombin and α1-antitrypsin was used for nickel sections. Briefly, sections were rinsed and blocked in blocking solution (0.1% Tween-TBS, 10% fetal calf serum, 5% bovine serum albumin) for 45 minutes and incubated with rabbit anti-human antithrombin and α1-antitrypsin polyclonal antibodies (1:250, Dako Diagnostics) for 90 minutes. Then, sections were washed three times in 0.1% Tween-TBS and incubated with 10 nm of protein A-conjugated colloidal gold in Tween-TBS (1:40) (Sigma-Aldrich). Nickel grid sections were then postfixed with osmium tetroxide and stained with uranyl acetate and lead citrate. Immunogold labeling was analyzed with the EM-10 Zeiss transmission electron microscope (Zeiss).

Statistical Analysis

Results are presented as mean values ± SD. Unpaired Mann-Whitney nonparametric *t*-tests were used for statistical significance determination purposes. Statistics were performed using GraphPad Prism, version 4.0 (San Diego, CA). A P value <0.05 was considered as statistically significant.

Results

ASNase Reduced the Anticoagulant Activity and Antigenic Levels of Antithrombin in ALL Patients

Induction ASNase treatment of ALL patients caused a rapid and severe reduction in the anticoagulant activity of antithrombin (Figure 1A). The average maximal loss of antithrombin achieved during ASNase treatment was 40.0 ± 10.6% of baseline values (range, 21.5 to 63.6) (Figure 1B). These results were similar to those observed in other studies.[12–19] Moreover, in all cases ASNase caused a type I deficiency, as activity and antigen displayed similar reductions (Figure 1C). However, once the treatment was stopped, antithrombin levels reached baseline values (Figure 1C). Thus, the induction treatment of ALL patients with ASNase determines an acquired but severe type I deficiency of antithrombin, similar to that observed in patients carrying heterozygous mutations, which explains the high thrombotic risk of these patients. In our study, two patients developed venous thrombosis in this period (10.5%). Interestingly, the thrombotic events take place when antithrombin levels were minimal (29.1% and 38.6% of basal values). SDS-PAGE and native Western blots of plasma samples of ALL patients under ASNase treatment revealed neither abnormal conformations nor significant increase of the latent form (data not shown).

In Vitro *Incubation with ASNase Had Neither Effect on Antithrombin Activity and Antigenic Levels nor on Conformation*

To test the direct effect of ASNase on antithrombin, plasma samples from healthy donors ($n = 4$) were incubated at 37°C up to 72 hours with ASNase (up to 700 IU/ml, which represents 10 times the amount of ASNase estimated in plasma of ALL patients under induction treatment) or sterile PBS. *In vitro* ASNase treatment of these samples affected neither the antigen levels of antithrombin nor its anti-FXa anticoagulant activity. Moreover, this incubation did not modify the electrophoretic mobility of the molecule in reduced SDS-PAGE. Additionally, it neither increased the levels of latent form nor produced polymers, and it had no effect on the heparin affinity of antithrombin. Similar results were observed when human purified antithrombin was used (at concentrations ranging from 150 μg/ml to 12 mg/ml) (data not shown).

ASNase Treatment Induced the Intracellular Accumulation and Concomitant Reduction in the Secretion of Antithrombin in HepG2 Cells

A previous study reported that ASNase treatment does not reduce antithrombin mRNA levels.[20] Accordingly, the decrease in plasma levels of antithrombin, as a consequence of the ASNase treatment, could be attributable to either posttranslational or secretory mechanisms. To as-

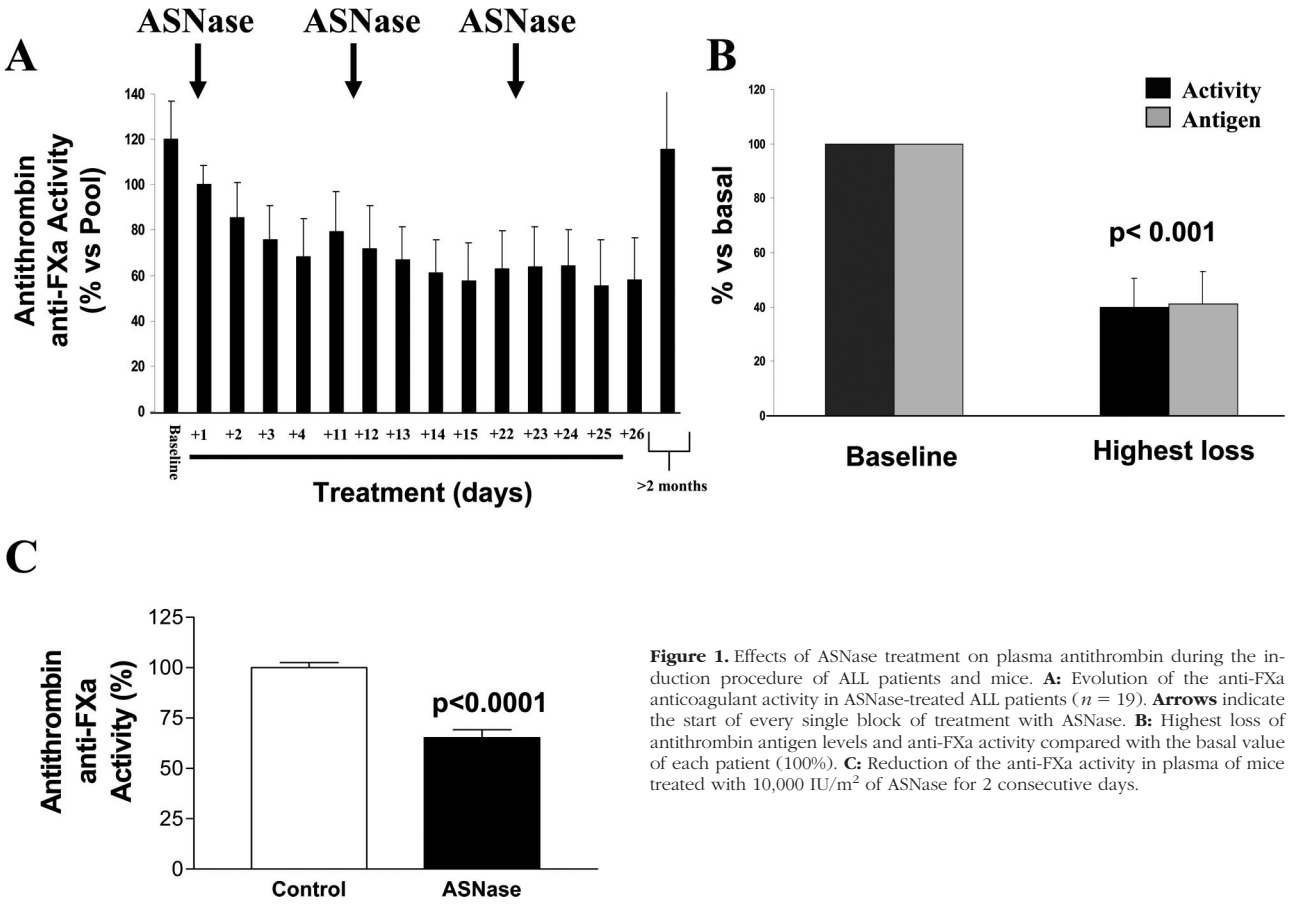

Figure 1. Effects of ASNase treatment on plasma antithrombin during the induction procedure of ALL patients and mice. **A:** Evolution of the anti-FXa anticoagulant activity in ASNase-treated ALL patients ($n = 19$). **Arrows** indicate the start of every single block of treatment with ASNase. **B:** Highest loss of antithrombin antigen levels and anti-FXa activity compared with the basal value of each patient (100%). **C:** Reduction of the anti-FXa activity in plasma of mice treated with 10,000 IU/m^2 of ASNase for 2 consecutive days.

sess any possible effect of ASNase treatment on antithrombin secretion, human hepatoma HepG2 cells were treated with either ASNase or sterile PBS. Concentrations of ASNase used to treat the cells were bioequivalent to those found in plasma of ALL patients treated with this drug (70 IU/ml). ASNase treatment produced a significant decrease ($P = 0.0031$) in the levels of antithrombin secreted to the medium by HepG2 cells (Figure 2A). This effect correlated with significant morphological changes in the cells. Indeed, untreated HepG2 cells had a round shape, cells were basophilic, with a foamy-like appearance, and their nuclei were homochromatinic. At 24 hours after ASNase treatment cells became fusiform, cytoplasms acquired a vacuolized appearance, and nuclei became more heterochromatinic (data not shown). Hoechst staining revealed decreased cell viability in ASNase-treated cells only after 48 hours (data not shown).

In parallel to these changes, we observed a significant intracellular accumulation of antithrombin. First, SDS-PAGE immunoblotting of cellular lysates revealed an increased proportion of intracellular antithrombin in treated cells (Figure 2B). Second, immunofluorescent labeling of antithrombin revealed the relocalization of the widespread diffuse antithrombin into more intense clusters (Figure 2C), suggestive of aggregates. Indeed, some of these clusters were Congo Red-positive (data not shown). Third, proteomic analysis confirmed the intracellular accumulation of antithrombin in ASNase-treated cells and revealed that ASNase treatment caused a modification on intracellular antithrombin because these molecules displayed different features increasing the pI of some forms and the amount of aggregated or polymeric forms (Figure 2D). Interestingly, a recent article found that antithrombin α and β forms (the last lacks the carbohydrate side chain on Asn^{135}) differ by ~0.135 pH units, assuming that the increase of the pI in the β form corresponds to different numbers of sialic acids at the end of carbohydrate antennas.[21] Therefore, antithrombin pI variations observed in this experiment might correspond to different carbohydrate contents of the molecule, but further experiments are required to characterize the post-translational modifications or abnormal conformations of antithrombin produced under ASNase treatment.

ASNase Treatment Caused a Significant Retention of Antithrombin in Livers of Mice, Which Determined a Circulating Acquired Type I Deficiency

The mouse model accurately reproduced the effects of ASNase treatment in ALL patients. Indeed, plasma of mice treated with ASNase revealed a decrease in antithrombin anti-coagulant activity (Figure 1C). Similarly to the results observed in HepG2 cells, ASNase treatment altered the morphology of the hepatocytes, by inducing

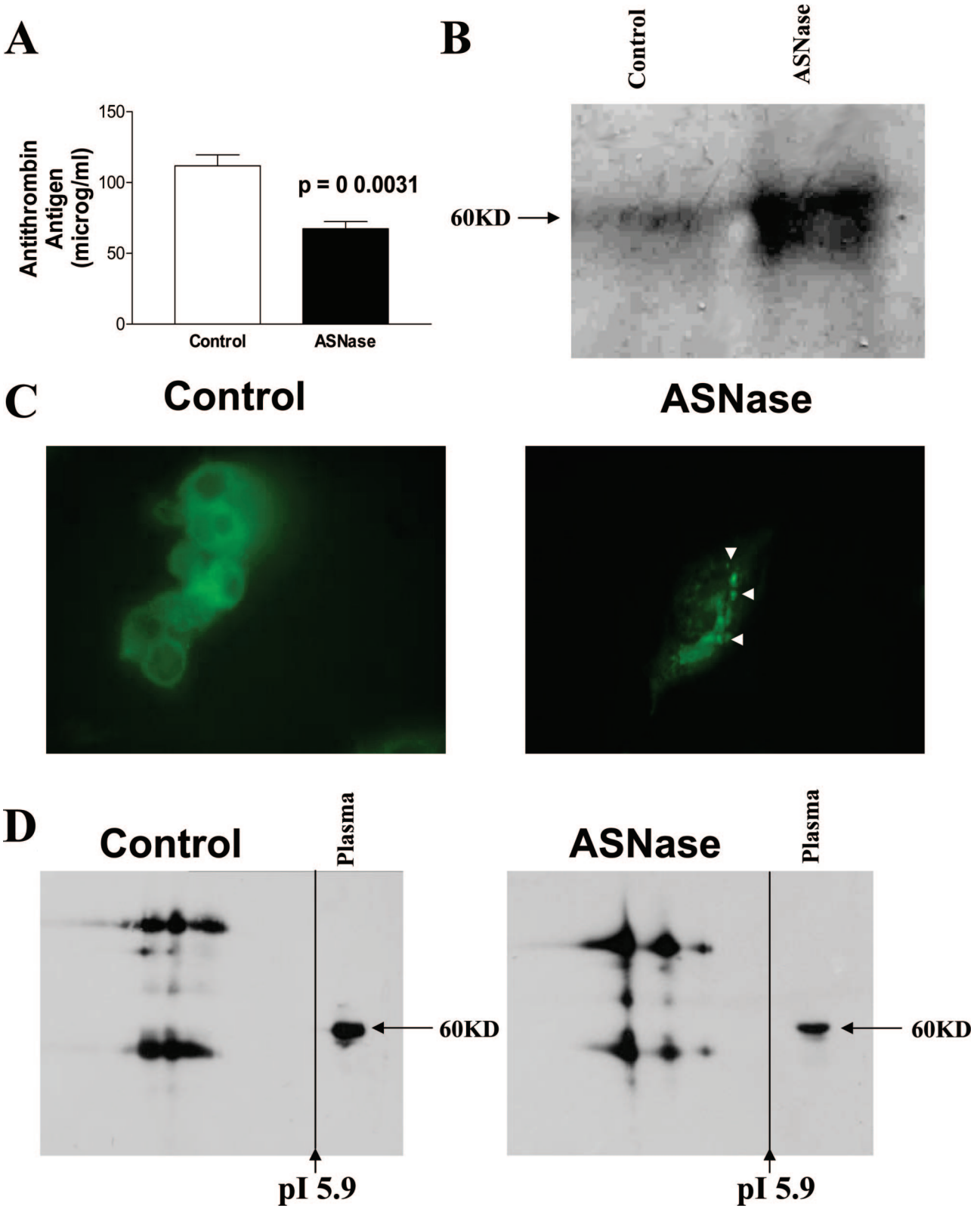

Figure 2. Effect of ASNase incubation of HepG2 cells after 24 hours. **A:** Antithrombin secreted to the medium as determined by enzyme-linked immunosorbent assay. **B:** Intracellular antithrombin of HepG2 lysates as evaluated by SDS-PAGE under reducing conditions and immunoblotting. **C:** Intracellular distribution of antithrombin in HepG2 as revealed by immunofluorescence. **Arrowheads** mark antithrombin aggregates. **D:** Antithrombin immunoblot of HepG2 immunoprecipitates after two-dimensional electrophoresis. Original magnifications, ×100 (**C**).

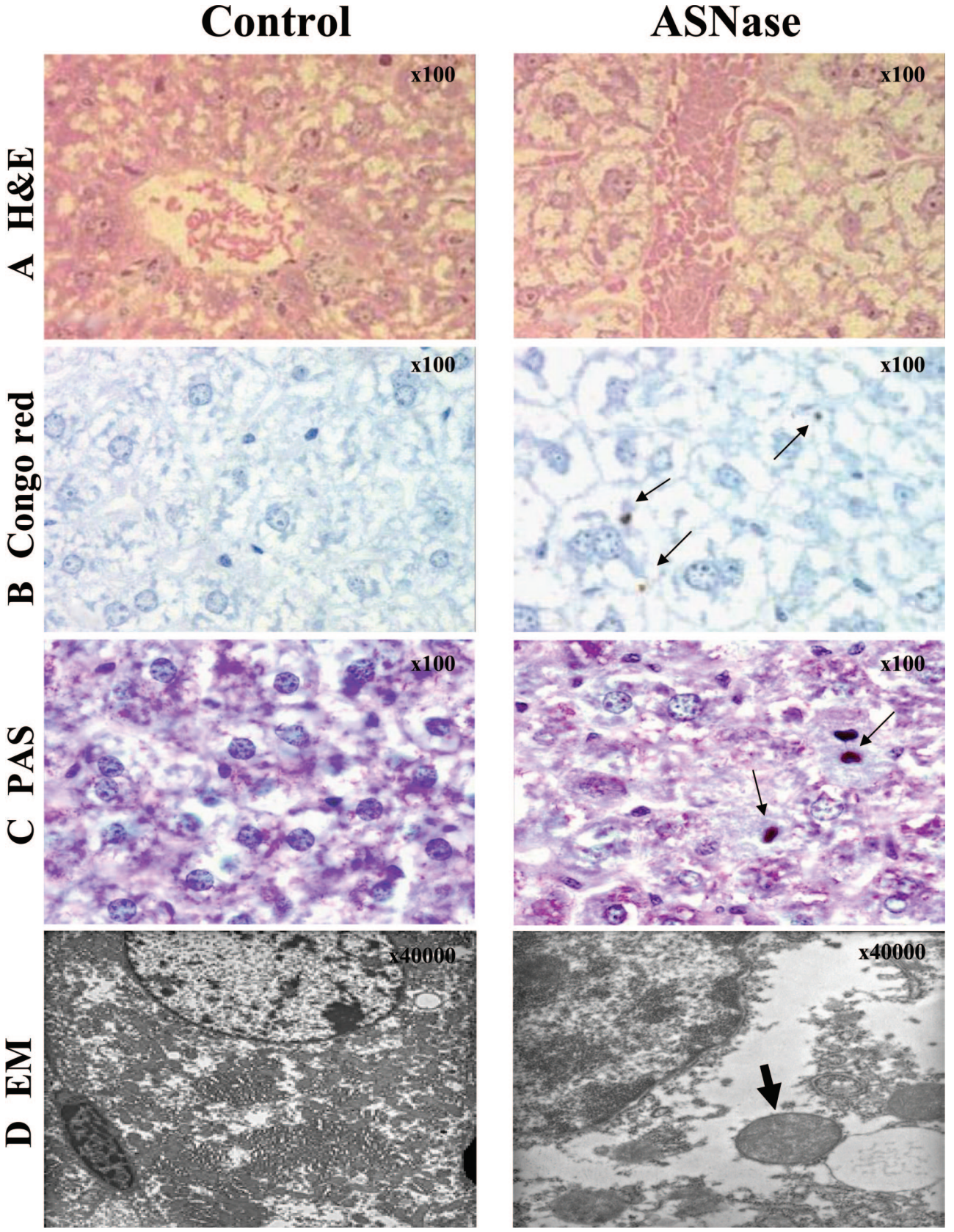

Figure 3. Consequences of ASNase treatment on mouse (2 days with 10,000 IU/m^2) livers and hepatocyte morphology as revealed by H&E (**A**), Congo Red (**B**), and PAS (**C**) staining under light microscopy, and by electronic microscopy (EM) (**D**). **Arrows** indicate intracellular aggregates of proteins. We point out the Mallory body-looking inclusion within the ER observed by EM (**bold arrow**). Original magnifications: ×100 (**A–C**); ×40,000 (**D**).

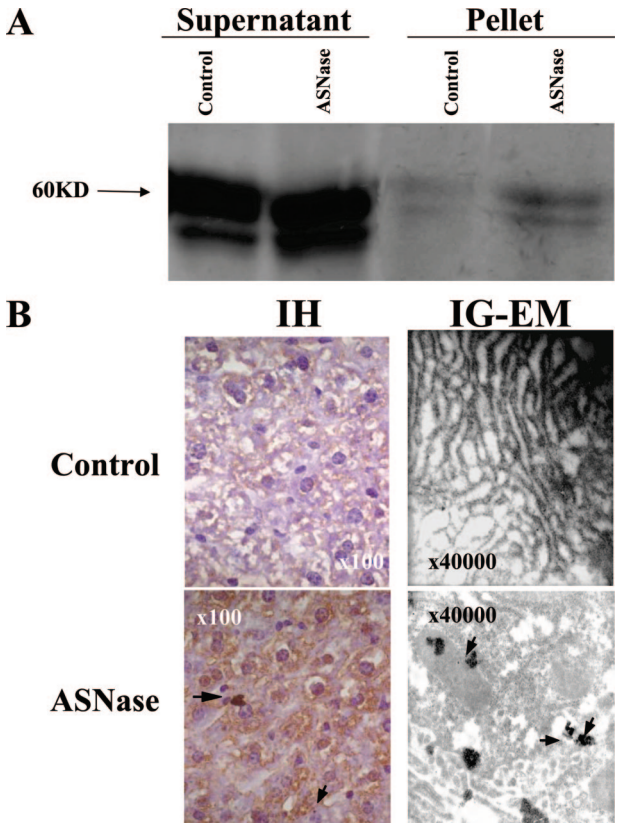

Figure 4. Intracellular retention of antithrombin aggregates in mice treated with ASNase (2 days with 10,000 IU/m^2). **A:** Intracellular antithrombin evaluated by SDS-PAGE under reducing conditions and immunoblotting of supernatant and pellets from liver lysates. **B:** Intracellular distribution of antithrombin and cellular morphology and ultrastructure of hepatocytes as revealed by immunohistochemistry (IH) under light microscopy and immunogold labeling electron microscopy (IG-EM). **Arrows** indicate antithrombin accumuli. Original magnifications: ×100 (**B**, **left**); ×40,000 (**B**, **right**).

intracellular depletion of glycogen and massive vacuolar degeneration by 24 hours after treatment (Figure 3A). Some of these vesicles contained Congo Red (Figure 3B) as well as periodic acid-Schiff (PAS)-positive deposits (Figure 3C), although cell death was not observed at this time point. Additionally, electron microscopy studies of livers from ASNase-treated mice revealed massive dilation of the rough endoplasmic reticulum (ER) cisterns and vacuoles that contained an electrodense material, some of them having Mallory body-looking appearance (Figure 3D).

Accordingly, we evaluated a possible intracellular retention and aggregation of antithrombin in livers of mice treated with ASNase. SDS-PAGE immunoblotting of cell lysates revealed intracellular accumulation of antithrombin, particularly insoluble material, as demonstrated by the increased amount of antithrombin in the pellets of ASNase-treated animals (Figure 4A). Moreover, immunohistochemistry studies showed an intracellular retention and aggregation of antithrombin in ASNase-treated mice (Figure 4B). Finally, immunogold labeling confirmed the retention and aggregation of the protein within the lumen of dilated rough ER cisterns of ASNase-treated mice (Figure 4B).

Effects of ASNase Treatment on α1-Antitrypsin

Similarly to antithrombin, patients under ASNase treatment also displayed a significant reduction in the plasma levels of α1-antitrypsin (Figure 5A). Moreover, ASNase treatment induced similar retention and intracellular aggregation of α1-antitrypsin to that seen for antithrombin in cells and livers of mice. Thus, immunofluorescence analysis of HepG2 cells showed an intense expression of α1-antitrypsin in a cluster-like pattern in ASNase-treated cells (Figure 5B). ASNase-treated mice displayed an increase in intracellular α1-antitrypsin (Figure 5C). Finally, immunohistochemical and immunogold-labeling electron microscopy studies also revealed the intracellular retention and aggregation of α1-antitrypsin within the lumen of dilated ER cisterns in livers of ASNase-treated mice (Figure 5D).

ASNase Treatment Induced Intracellular Retention and Accumulation of Glycoproteins in Other Tissues

Additionally, we observed that ASNase treatment had a more widespread action on conformationally-sensitive tissues such as the pancreas and central nervous system. Thus, scattered Congo Red- and PAS-positive intracytoplasmic deposits of proteins were found in pancreas (Figure 6A) and white matter from frontal cortex in ASNase-treated mice (Figure 6B).

Discussion

Conformational diseases constitute an important group of disorders, including diseases such as Alzheimer's disease, Huntington's disease, familial dementia, emphysema, Creutzfeld-Jakob disease/scrapie, bovine spongiform encephalopathy, Parkinson's disease, or type 2 diabetes mellitus, among others.[22] Most of these disorders affect proteins with a certain degree of conformational instability. Thus, mutations affecting the structure of the protein or noxious stimuli enable proteins to adopt a partially folded state. In a second step, this intermediate conformer forms intermolecular bonds that lead to multimeric structures, a step often mediated via hydrophobic or β-strand interactions, which culminate in the deposition of proteinaceous aggregates.[23] Although a wide variety of clinical presentations and triggering factors exist, understanding the pathological mechanism for one of these diseases might help to unravel the mechanisms involved in the pathogenesis of the others. Moreover, similar therapeutical approaches might be applied to different diseases.[23] Interestingly, many of the conformational diseases are caused by abnormal aggregation of serpins.[24] Certainly, the molecular flexibility of serpins, which is necessary for their inhibitory function, also renders these molecules especially susceptible to even minor changes.[2] Point mutations in the mobile domains of several serpins, such as α1-antitrypsin, C1-inhibitor of complement, or neuroserpin, make the molecule vulner-

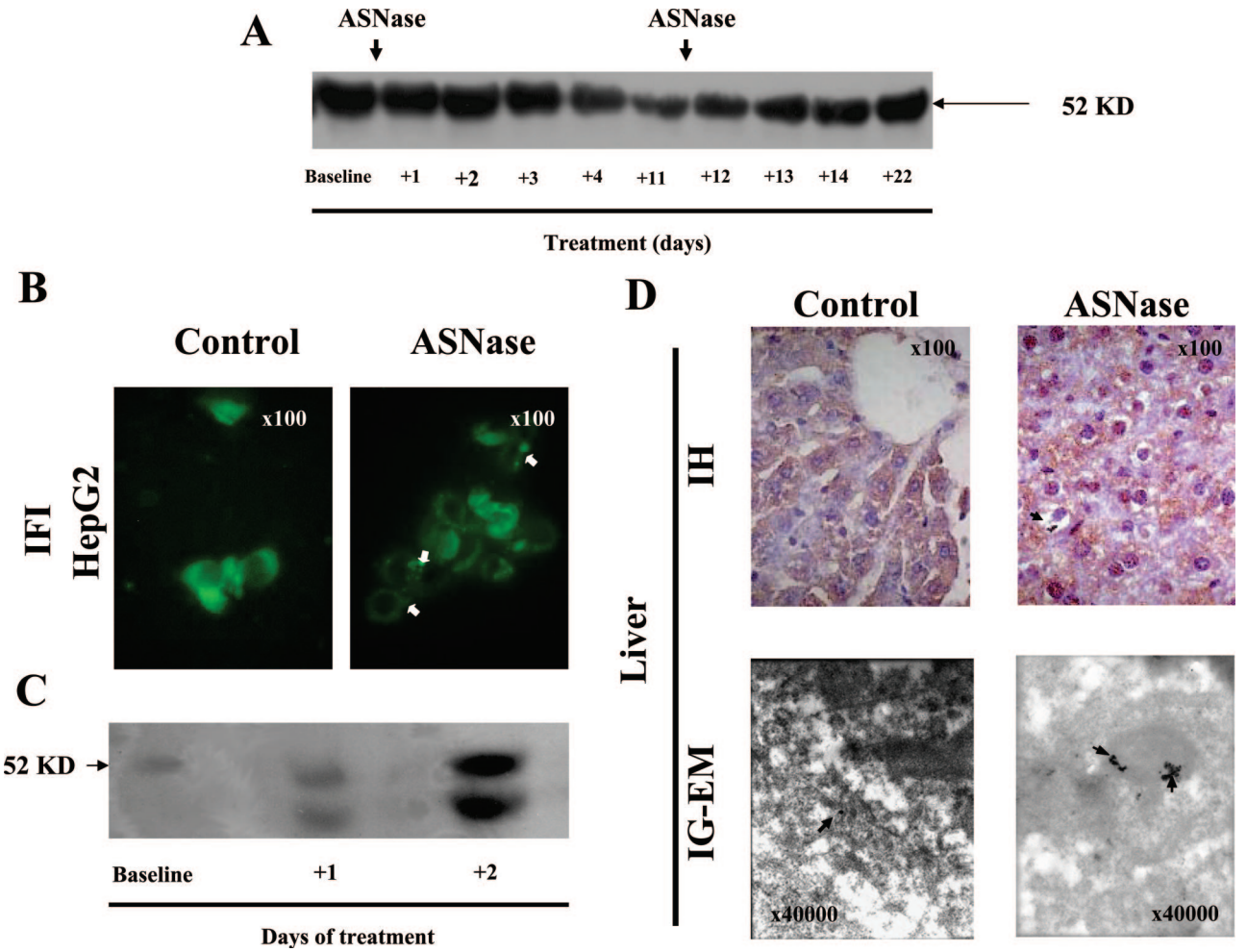

Figure 5. Effects of ASNase on α1-antitrypsin secretion and retention. **A:** Effects of ASNase treatment on the levels of α1-antitrypsin in plasma during the induction procedure of ALL patients. **B:** Intracellular retention and aggregation of α1-antitrypsin in HepG2 cells as revealed by immunofluorescence (IF) after 24 hours of incubation with ASNase. **C** and **D:** Intracellular α1-antitrypsin in livers of ASNase-treated mice (2 days with 10,000 IU/m^2) and their control littermates, as revealed by immunoblotting of supernatants from liver lysates (**C**) and by immunohistochemistry (IH) under light microscopy or immunogold-labeling and electron microscopy (IG-EM) (**D**). **Arrows** indicate α1-antitrypsin aggregates. Original magnifications: ×100 [**B**, **D** (**top**)]; ×40,000 (**D**, **bottom**).

able to aberrant conformational transitions that allow protein polymerization at cell synthesis and processing stages.[24] This has two relevant consequences. First, their secretion becomes impaired causing a plasma deficiency, which could have pathological consequences (such as emphysema or angioedema). Second, accumulation of polymers inside cells might be toxic, leading to cell death or degeneration that is also associated with diseases such as cirrhosis or dementia.[24,25]

Antithrombin has also been involved in conformational diseases (T. Bayston, D. Lane: Antithrombin mutation database. Department of Haematology, Imperial College Faculty of Medicine, Charing Cross Hospital Campus, Hammersmith, London, UK. *http://www1.imperial.ac.uk/medicine/about/divisions/is/haemo/antithrombin/default.html*).[3,4] Particular missense mutations cause dimerization, trimerization, or polymerization and intracellular retention.[4] Environmental factors also cause conformational modifications in antithrombin. Particularly, high temperatures (>60°C) or low pH (<6.5) induce the formation of antithrombin polymers *in vitro*.[8,11,26] However, some of these conditions can hardly be achieved under pathophysiological situations. Herein, we show consistent data supporting the first evidence that the drug ASNase causes an acquired and transient but profound deficit of antithrombin, probably through a conformational mechanism, which increases the risk of thrombosis. In fact, two ASNase-treated ALL patients developed deep venous thrombosis in the course of this study.

L-Asparaginase (EC 3.5.1.1) hydrolyzes L-asparagine to L-aspartate and ammonia. ASNase activity might directly affect key asparagine (Asn) residues of the molecule. Three Asn are conserved in >70% of serpins—Asn 49, 158, and 186 in α1-antitrypsin numbering, supporting their structural relevance.[27] Moreover, three mutations affecting the antithrombin gene changed two Asn residues, one strongly conserved, Asn 187 (Asn 158 in the α1-antitrypsin template) that is mutated to Lys or Asp, and Ans405Lys (T. Bayston, D. Lane: Antithrombin mutation database. Department of Haematology, Imperial College Faculty of Medicine, Charing Cross Hospital Campus, Hammersmith, London, UK. *http://www1.imperial.ac.uk/medicine/about/divisions/is/haemo/antithrombin/default.html*). These mutations caused type II deficiency (T. Bayston, D. Lane: Antithrombin muta-

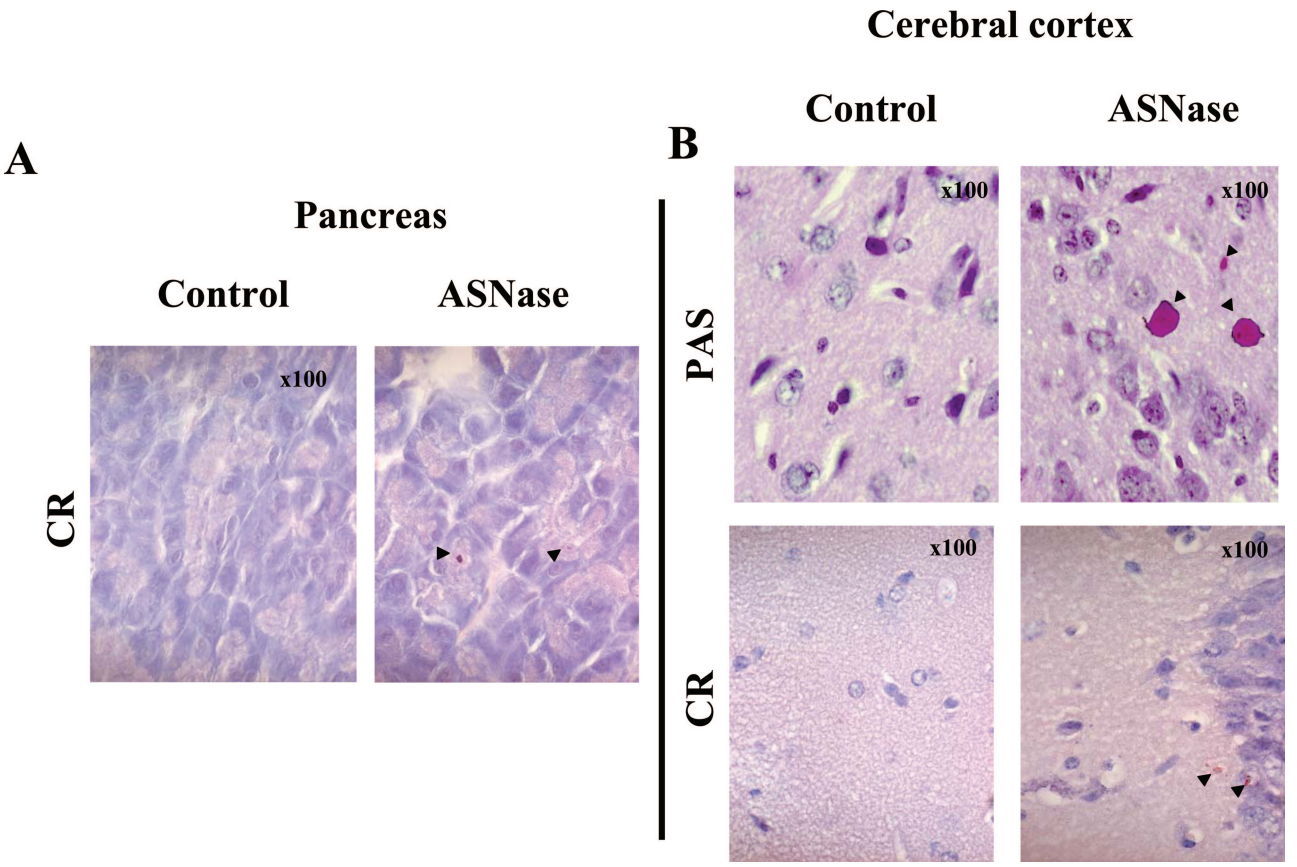

Figure 6. Intracellular accumulation of proteins in pancreatic acinar cells (**A**) and frontal cortex white matter (**B**) from mice treated with ASNase (2 days with 10,000 IU/m^2), as revealed by Congo Red and PAS staining under light microscopy. **Arrowheads** indicate β-amyloid (**A**, **B**) and glycoprotein (**B**) deposits. Original magnifications, ×100.

tion database. Department of Haematology, Imperial College Faculty of Medicine, Charing Cross Hospital Campus, Hammersmith, London, UK. *http://www1.imperial.ac.uk/medicine/about/divisions/is/haemo/antithrombin/default.html*). Interestingly, the mutation of the conserved Asn 187 to Asp (antithrombin Rouen-VI) in the F-helix destabilizing the underlying A-sheet of the molecule causes an increased rate of peptide insertion into the A-sheet, facilitating the formation of polymers.[9] Accordingly, ASNase could directly cause conformational changes in antithrombin molecules by modifying these Asn residues. However, our *in vitro* experiments support that the enzymatic activity of ASNase has no effect on the mature secreted protein, affecting neither its conformation nor activity. In contrast, this drug caused a transient but potent retention of this molecule within ER cisterns and vacuoles, which explains the severe type I deficiency observed in cell culture, mice, and patients. Remarkably, this effect is not specific to antithrombin. We have also demonstrated similar effects on α1-antitrypsin, another hepatic serpin, probably affecting other structurally flexible proteins, as suggested by Congo Red and PAS stainings. Additionally, these effects could not be restricted to the liver but affected other cell types in which conformational diseases are promiscuous, such as pancreatic acinar cells or neurons.

Our results suggest that the effects of ASNase are restricted to the nascent molecules at the intracellular level. Different hypotheses could explain the ASNase-induced intracellular mechanism. First, although the ASNase used in ALL therapy belongs to the high-affinity variants (type II), further enhancement of activity of the intracellular L-asparaginase Gliap, an atypical type I L-asparaginase particularly abundant in liver,[28] could affect Asn residues of the nascent proteins. These residues are required for accurate glycosylation and are therefore critical for proper folding, especially of conformationally sensitive proteins, such as antithrombin or α1-antitrypsin. On the other hand, high ammonia levels, such as those observed under ASNase treatment,[29] have been shown to interfere at different points with the intracellular energy metabolism and to produce oxidative stress.[30] Metabolic energy is necessary for the proper folding of proteins as well as for the degradation of misfolded proteins.[31] Additionally, oxidation per se can interfere with the proper folding of proteins. Certain oxidized proteins are poorly handled and become accumulated.[32] Moreover, the ability of a cell to deal with reactive oxygen species and oxidative stress depends on a cascade of intracellular events collectively known as the unfolded protein response, which includes chaperone up-regulation, antioxidant production, and protein degradation. The liver is particularly susceptible to perturbations in this quality control system. Indeed, different insults favor the formation of inclusion bodies known as Mallory bodies.[33–35]

Therefore, high ammonia levels could lead to intracellular accumulation of particularly susceptible proteins. Further experiments are required to confirm the exact mechanism that causes the intracellular accumulation of proteins during ASNase treatment.

In the course of normal protein biosynthesis, misfolding does occur especially in conformationally sensitive molecules such as serpins. Accordingly, intracellular mechanisms have evolved to degrade these aberrant proteins.[36] A particular protein susceptibility to aggregation, caused by genetic or environmental factors, may overwhelm the quality control mechanisms of the cell. In this setting, ER quality control mechanisms can prove insufficient. High concentrations of mutant proteins lead to aggregation and slow deposition into tissues throughout time, explaining the late onset of many conformational diseases. However, during the ASNase treatment, ER stress is transient, and the main pathological consequence becomes an impaired secretion of proteins, causing a circulating deficiency. For antithrombin, such acquired deficiency, even when transient, significantly increases the risk of thrombosis. Two simple adaptive mechanisms are used to bring the folding capacity of the ER and its unfolded protein burden and return the ER to its normal physiological state: up-regulation of the folding capacity of the ER through induction of ER-resident molecular chaperones and foldases and an increase in the size of the ER and down-regulation of the biosynthetic load of the ER through shut-off of protein synthesis at transcriptional and translational levels and increased clearance of unfolded proteins from the ER through up-regulation of ER-associated degradation.[37] During ASNase treatment, we observed an increase in the size of the ER, suggesting the activation of these protective mechanisms. Thus, after ASNase treatment, these mechanisms will probably remedy the stress situation, and apoptosis is not initiated, even if highly expressed proteins are affected. However, ASNase treatment might impair the function of the affected organs, especially if combined with additional factors. Therefore, adverse side effects of this treatment such as hepatotoxicity and neurotoxicity can be at least partially explained by the conformational effects of ASNase treatment on organs that are particularly susceptible to conformational diseases.

In summary, ASNase affects neither functional nor conformational parameters of the circulating pool of antithrombin but causes a severe yet transient type I antithrombin, deficiency that justifies the increased risk of thrombosis seen in ALL patients. This effect is a consequence of impaired secretion due to intracellular aggregation within the ER cisterns and vacuoles, forming in some cases crystalloid structures that are similar to inclusion bodies. Features of these aggregates of antithrombin are similar to those observed in the Z-form of α1-antitrypsin produced by the mutation Glu342Lys.[25] These data support the first case of a nonmutational conformational mechanism that causes antithrombin deficiency. Other factors yet to be defined might have similar consequences and therefore could be involved in acquired deficiency of this potent anticoagulant or other diseases by means of an acquired conformational mechanism.

Acknowledgments

We thank Dr. M.M. Bermúdez, M.E. Linares (Servicio de Oncología Pediátrica, Hospital Virgen de la Arrixaca, Murcia, Spain), and H. Cano (Servicio de Hematología, Hospital Comarcal los Arcos, Murcia, Spain) for the collection of samples and clinical data of patients.

References

1. Ishiguro K, Kojima T, Kadomatsu K, Nakayama Y, Takagi A, Suzuki M, Takeda N, Ito M, Yamamoto K, Matsushita T, Kusugami K, Muramatsu T, Saito H: Complete antithrombin deficiency in mice results in embryonic lethality. J Clin Invest 2000, 106:873–878
2. Carrell RW, Huntington JA: How serpins change their fold for better and for worse. Biochem Soc Symp 2003, 70:163–178
3. Carrell RW, Huntington JA, Mushunje A, Zhou A: The conformational basis of thrombosis. Thromb Haemost 2001, 86:14–22
4. Corral J, Vicente V, Carrell RW: Thrombosis as a conformational disease. Haematologica 2005, 90:238–246
5. Wriston Jr JC, Yellin TO: L-Asparaginase: a review. Adv Enzymol Relat Areas Mol Biol 1973, 39:185–248
6. Athale UH, Chan AK: Thrombosis in children with acute lymphoblastic leukemia. Part III. Pathogenesis of thrombosis in children with acute lymphoblastic leukemia: effects of host environment. Thromb Res 2003, 111:321–327
7. De Stefano V, Sora F, Rossi E, Chiusolo P, Laurenti L, Fianchi L, Zini G, Pagano L, Sica S, Leone G: The risk of thrombosis in patients with acute leukemia: occurrence of thrombosis at diagnosis and during treatment. J Thromb Haemost 2005, 3:1985–1992
8. Zhou A, Huntington JA, Carrell RW: Formation of the antithrombin heterodimer in vivo and the onset of thrombosis. Blood 1999, 94:3388–3396
9. Bruce D, Perry DJ, Borg JY, Carrell RW, Wardell MR: Thromboembolic disease due to thermolabile conformational changes of antithrombin Rouen-VI (187 Asn–>Asp). J Clin Invest 1994, 94:2265–2274
10. Mushunje A, Evans G, Brennan SO, Carrell RW, Zhou A: Latent antithrombin and its detection, formation and turnover in the circulation. J Thromb Haemost 2004, 2:2170–2177
11. Corral J, Rivera J, Martinez C, Gonzalez-Conejero R, Minano A, Vicente V: Detection of conformational transformation of antithrombin in blood with crossed immunoelectrophoresis: new application for a classical method. Lab Clin Med 2003, 142:298–305
12. Anderson N, Lokich JJ, Tullis JL: L-Asparaginase effect on antithrombin-III levels. Med Pediatr Oncol 1979, 7:335–340
13. Vellenga E, Mulder NH, Nieweg HO: Antithrombin III deficiency during asparaginase therapy. Lancet 1980, 1:649–650
14. Bauer KA, Teitel JM, Rosenberg RD: L-asparaginase induced antithrombin III deficiency: evidence against the production of a hypercoagulable state. Thromb Res 1983, 29:437–442
15. Liebman HA, Wada JK, Patch MJ, McGehee W: Depression of functional and antigenic plasma antithrombin III (AT-III) due to therapy with L-asparaginase. Cancer 1982, 50:451–456
16. Andrew M, Brooker L, Mitchell L: Acquired antithrombin III deficiency secondary to asparaginase therapy in childhood acute lymphoblastic leukaemia. Blood Coagul Fibrinolysis 1994, 5(Suppl 1):S24–S64
17. Mitchell L, Hoogendoorn H, Giles AR, Vegh P, Andrew M: Increased endogenous thrombin generation in children with acute lymphoblastic leukemia: risk of thrombotic complications in L'asparaginase-induced antithrombin III deficiency. Blood 1994, 83:386–391
18. Nowak-Gottl U, Boos J, Wolff JE, Lill H, Veltmann H, Werber G, Ahlke E, Jurgens H: Asparaginase decreases clotting factors in vitro: a possible pitfall? Int J Clin Lab Res 1995, 25:146–148
19. Nowak-Gottl U, Ahlke E, Fleischhack G, Schwabe D, Schobess R, Schumann C, Junker R: Thromboembolic events in children with

acute lymphoblastic leukemia (BFM protocols): prednisone versus dexamethasone administration. Blood 2003, 101:2529–2533
20. Bushman JE, Palmieri D, Whinna HC, Church FC: Insight into the mechanism of asparaginase-induced depletion of antithrombin III in treatment of childhood acute lymphoblastic leukemia. Leuk Res 2000, 24:559–565
21. Kremser L, Bruckner A, Heger A, Grunert T, Buchacher A, Josic D, Allmaier G, Rizzi A: Characterization of antithrombin III from human plasma by two-dimensional gel electrophoresis and capillary electrophoretic methods. Electrophoresis 2003, 24:4282–4290
22. Carrell RW, Lomas DA: Conformational diseases. Lancet 1997, 350:134–138
23. Chow MK, Lomas DA, Bottomley SP: Promiscuous beta-strand interactions and the conformational diseases. Curr Med Chem 2004, 11:491–499
24. Lomas DA, Carrell RW: Serpinopathies and the conformational dementias. Nat Rev Genet 2002, 3:759–768
25. Carrell RW, Lomas DA: α1-Antitrypsin deficiency: a model for conformational diseases. N Engl J Med 2002, 346:45–53
26. Zhou A, Stein PE, Huntington JA, Carrell RW: Serpin polymerization is prevented by a hydrogen bond network that is centered on his-334 and stabilized by glycerol. J Biol Chem 2003, 278:15116–15122
27. Irving JA, Pike RN, Lesk AM, Whisstock JC: Phylogeny of the serpin superfamily: implications of patterns of amino acid conservation for structure and function. Genome Res 2000, 10:1845–1864
28. Dieterich DC, Landwehr M, Reissner C, Smalla KH, Richter K, Wolf G, Bockers TM, Gundelfinger ED, Kreutz MR: Gliap—a novel untypical L-asparaginase localized to rat brain astrocytes. J Neurochem 2003, 85:1117–1125
29. Laterza OF, Gerhardt G, Sokoll LJ: Measurement of plasma ammonia is affected in patients receiving asparaginase therapy. Clin Chem 2003, 49:1710–1711
30. Norenberg MD, Rama Rao KV, Jayakumar AR: Ammonia neurotoxicity and the mitochondrial permeability transition. J Bioenerg Biomembr 2004, 36:303–307
31. Yano M, Kanesaki Y, Koumoto Y, Inoue M, Kido H: Chaperone activities of the 26S and 20S proteasome. Curr Protein Pept Sci 2005, 6:197–203
32. Dean RT, Fu S, Stocker R, Davies MJ: Biochemistry and pathology of radical-mediated protein oxidation. Biochem J 1997, 324:1–18
33. Stumptner C, Fuchsbichler A, Heid H, Zatloukal K, Denk H: Mallory body—a disease-associated type of sequestosome. Hepatology 2002, 35:1053–1062
34. French BA, van Leeuwen F, Riley NE, Yuan QX, Bardag-Gorce F, Gaal K, Lue YH, Marceau N, French SW: Aggresome formation in liver cells in response to different toxic mechanisms: role of the ubiquitin-proteasome pathway and the frameshift mutant of ubiquitin. Exp Mol Pathol 2001, 71:241–246
35. Mori S, Yamasaki T, Sakaida I, Takami T, Sakaguchi E, Kimura T, Kurokawa F, Maeyama S, Okita K: Hepatocellular carcinoma with nonalcoholic steatohepatitis. J Gastroenterol 2004, 39:391–396
36. Goldberg AL: Protein degradation and protection against misfolded or damaged proteins. Nature 2003, 426:895–899
37. Schroder M, Kaufman RJ: ER stress and the unfolded protein response. Mutat Res 2005, 569:29–63